Uludağ University Journal of The Faculty of Engineering, Vol. 23, No. 3, 2018 RESEARCH

DOI: 10.17482/uumfd.455326

DEVELOPMENT OF A PHASE-OTDR INTERROGATOR BASED ON COHERENT DETECTION SCHEME

Kıvılcım YÜKSEL [*]
Johan JASON [**]
Marc WUILPART [**]

Received: 08.08.2018; revised:14.11.2018; accepted: 14.12.2018

Abstract: We present in this work, the experimental demonstration of a phase-sensitive Optical Time-Domain Reflectometer (phase-OTDR) having coherent detection scheme. An analysis algorithm has also been developed to calculate amplitude and phase evolution of the experimental phase-OTDR traces. The efficiency of the analysis algorithm to determine the position of the applied vibration has been verified for a single and two simultaneous vibrations. The slow-time analysis results show a good agreement with the mathematical calculations discussed in the paper. This work could have a technological implication in many fields such as distributed vibration sensor for railway monitoring applications.

Keywords: Coherent detection, Phase-OTDR, Fiber optic sensor

Evreuyumlu Algılama Tabanı Faz-OTDR Sorgulayıcı Ünite Geliştirilmesi

Öz: Bu çalışmada, evre uyumlu algılayıcıya sahip bir faza duyarlı frekans bölgesinde optik yansıtıcı (faz-OTDR) ünitesi deneysel olarak gerçeklenmiştir. Faz-OTDR izlerine ait genlik ve faz cevaplarının hesaplanmasını sağlayan analiz algoritmaları geliştirilmiştir. Sözkonusu algoritmaların fiber üzerine tek veya aynı anda iki noktada titreşim uygulandığında, titreşim konum ve frekansını tespit kabiliyeti deneysel olarak gösterilmiştir. Yavaş-zaman analizleri ile elde edilen sonuçlar, makalede tartışılan matematiksel ispat ile uyumlu sonuç vermiştir. Makalede ele alınan sensör sorgulama ünitesi, dağıtık titreşim algılayıcılar kullanılarak trenyolu izleme sistemleri tasarımı gibi pek çok teknolojik alanda etki yaratma potansiyeli taşımaktadır.

Anahtar Kelimeler: Evreuyumlu algılama, Faz-OTDR, Fiber optic algılayıcı

1. INTRODUCTION

Distributed acoustic sensing (DAS) (also known as distributed vibration sensing, DVS) is a fiber-optic sensing technique based on the detection of Rayleigh backscattered (RBS) light in optical fibers using optical time domain reflectometry (OTDR). The OTDR technique used for DAS/DVS is called ϕ-OTDR (phase-OTDR) and has been a field of intensive research for more than ten years (Masoudi, et. al., 2017; Miah, et. al., 2017; Jason, et.al., 2018).

ϕ-OTDR is based on a pulsed laser source that must be highly coherent, contrary to conventional OTDR systems used as a maintenance and troubleshooting tool in optical fiber

[*] İzmir Institute of Technology, Electrical and Electronics Engineering Department, 35430, Urla, İzmir, Türkiye
[**] University of Mons, Faculty of Engineering, Electromagnetism and Telecommunication Department, 7000, Mons, Belgium

Corresponding author: Kıvılcım Yüksel (kivilcimyuksel@iyte.edu.tr)

communication cables, where low coherence is desired to minimize measurement noise. Among all the vibration sensing techniques, ϕ-OTDR has been given a growing attention because of its ability in the realization of spatially resolved measurements that are capable of both characterizing and localizing a vibration or acoustic phenomenon present along a long-distance optical fiber (Liu, et.al., 2016).

The single-mode optical fiber used as the sensing element for DAS is the same as the fiber used in telecom cables, which means that existing telecom cable installations can be used for sensing purposes. ϕ-OTDR based DAS systems owe their popularity to their remote sensing capability, that is, the sensing fiber can be placed along long and inaccessible spaces (e.g. underground pipes, oil wells, railways) while the interrogator unit is kept at a safe distance. The most common application proposed for this technique is intrusion monitoring (Taylor, et. al., 1993). Effectiveness of ϕ-OTDR have been demonstrated by various enhanced systems for detecting and locating intruders (Juarez, et. al., 2005, Olcer, et. al., 2017, Aktas, et.al., 2017, Maral, et.al., 2018). Other applications include oil well monitoring (Madsen, et. al., 2012), train and rail track monitoring (Wang, et. al., 2017, Jason, et.al., 2017).

ϕ-OTDR schemes can be divided into two main categories according to the detection method employed; namely, direct detection and coherent detection ϕ-OTDR. The straightforward direct detection scheme relies on the registration of local changes in the backscattered signal's power over time. With coherent detection, the backscattered signal is mixed with a reference signal, and the amplitude as well as the phase component of the backscattered signal can be extracted.

The backscattered signal power is not linearly related to the magnitude of the vibrations. Therefore, direct detection schemes provide information only about the frequency content of the vibration. Nevertheless, the extraction of phase can be used to deduce both the magnitude and frequency of external vibrations. Hence, the recent research papers related to ϕ-OTDR have been focusing more on the implementation of coherent detection schemes, rather than the well-established but relatively limited direct detection methods.

In this paper, different trends in ϕ-OTDR employing coherent detection have been first summarized (cf. Table 1). Then, a modified version of the heterodyne detection scheme presented in Pan et.al. (2011) has been experimentally demonstrated.

From the measured ϕ-OTDR traces, amplitude and phase information have been extracted. Amplitude evolution of the consecutively recorded ϕ-OTDR traces has been successfully used to locate the vibration locations. SNR values on the measured traces have also been calculated and compared for two different input signal levels. Afterwards, slow-time analysis has been applied on both the amplitude and the differential phases. Instead of extracting the vibration amplitudes, however, it was aimed in this paper, to compare slow-time analysis of the amplitude response and that of the phase difference with respect to the appearance of unwanted harmonic frequencies. Slow-time analysis of the phase difference has been shown to be more reliable in avoiding harmonics. This property of the coherent detection scheme can be considered as an important advantage in correctly interpreting the frequency response of the field measurements.

Lastly, we realized a mathematical demonstration of the theoretical limitations for the maximum vibration frequency that can be measured by the proposed set-up. Experimental results showed an excellent agreement with the theory that is elaborated in the paper.

Table 1. Classification of phase-OTDR using coherent detection scheme. SR: spatial resolution, ESA: Electrical Spectrum Analyzer, BPF: Band Pass Filter, LPF: Low Pass Filter, DSP: Digital Signal Processing

Reference	Added value of the work	Key component in the experimental implementation	Performance Parameters	Application Area
(Peng, et.al., 2014)	Implementation of Raman amplification	Optical BPF and ESA	SR of 8 m over 131 km measurement range SNR of 21 dB at 375 Hz vibration frequency.	Intrusion detection of pipelines
(Lu, et. al., 2010)	Implementation of moving averaging and moving differential signal processing methods	Electrical mixer, LPF	SR of 5 m. Maximum vibration frequency of 1 kHz	Early crack identification in concrete or steel structures (e.g. bridges)
(Pan, et. al., 2011)	Implementation of phase modulated paired pulse method	Data processing steps after acquisition	Vibration frequency of hundreds of Hz over about 1 km	Distributed vibration sensing
(He, et. al., 2016)	Self-mixing demodulation technique	Self-mixing demodulation system consisting of power divider, mixer, BPF, LPF	SR of 10 m over 42 km measurement range Vibration frequency range from 8 Hz to 980 Hz with SNR of 21.4 dB	Not reported
(Yu, et.al, 2017)	Single-source dual heterodyne detection scheme	Dual heterodyne detection system employing BPF, LPF, DSP module	SR of 9 m over 24.6 km SNR of 23.5 dB at vibration frequency range from 5 Hz to 1.715 kHz	Future engineering applications

2. EXPERIMENTAL SET UP

When a vibration of a certain frequency is applied on the sensor fiber at a particular position, this section of the fiber is dynamically strained which gives rise to a change of refractive index (strain-optic effect) and a change in relative positions of the scattering centers. As a result, the amplitude of the registered backscattered signal over time varies in response to the vibration. Hence, by subtracting two consecutive traces, one can localize the perturbation. However, the relation between the magnitude of vibration (acceleration) and the power of the registered backscattered light is not necessarily linear. This nonlinearity can be explained by two reasons. Firstly, the original fiber index distribution and scatterer positions are random. Secondly, even if they are known, the measured power and the phase are related through a nonlinear function (cosine). It is therefore necessary to implement coherent detection scheme permitting the extraction of phase difference between two locations in order to determine the vibration magnitude (Pan, et. al., 2011).

A coherent detection-based ϕ-OTDR set-up has been implemented in this work. The layout of the experimental ϕ-OTDR system is shown in Figure 1. The signal from the coherent laser source is divided into two parts by 90:10 coupler. One portion (acting as a probe signal) is modulated into optical pulses by an AOM having a certain pulse-width (τ) and Pulse Repetition Frequency (PRF). The optical frequency of the probe signal is also shifted (f_{AOM}). After amplifying (by an EDFA) and filtering (for the elimination of ASE noise), the probe signal is injected into the FUT through a circulator. The light wave scattered from individual scattering centres interfere coherently and the Rayleigh backscattered signal can be described as

$$E_{RBS}(t) = R(t)E_0 e^{j[2\pi(f+f_{AOM})t+\theta_R(t)]} \quad (1)$$

where f_{AOM} is the frequency shift imposed by AOM, E_0 is the amplitude of the probe pulse sent into FUT, f is the optical frequency, and $\theta_R(t)$ is the phase term representing the influence of the refractive index change along the fiber. Here, the pulse shape has been considered as perfectly rectangular and phase noise of the laser source is neglected.

A small portion (10%) of the CW laser signal (acting as a reference signal, or local oscillator, LO) is combined with the Rayleigh backscattered light wave using a 50:50 coupler which generates an interference signal at each output port of the coupler. These interference signals constitute a direct current (DC) term and an AC component resulting from the phase difference (due to AOM frequency shift) between the probe and the reference signals (LO). A balanced photodetector (BPD) is used to eliminate the DC term. The AC component of the beat signal taken from the output of the BDP is represented as

$$I(t) \propto R(t)E_0^2 \cos(\theta_p)\cos(2\pi f_{AOM}t + \theta_R(t)) \quad (2)$$

where the term $\cos(\theta_p)$ representing the polarisation mismatch between LO and RBS is assumed to be globally optimised by using the polarisation controller inserted in the reference path (cf. Figure 1). A polarisation diversity detection scheme is preferred for a complete elimination of this effect, as the state of polarisation changes along the fiber (i.e. $\cos(\theta_p)$ varies over the fiber length) (Ren, et. al., 2016).

A small part of the probe signal is converted into an electrical pulse and used as a trigger signal for the data acquisition. For each trigger, the electrical signal at the output of the balanced photodetector is acquired via the digitizer over the temporal interval determined by the PRF.

Each ϕ-OTDR trace of N samples is taken between these successive triggers (or pulses). The beat signal sampled at the digitizer at a given moment is the result of backscattering over

some limited zone, called '*spatial resolution cell*' whose spatial length is half the pulse-width. In the experiments, $N = 50000$ samples are taken by a digitizer with 1 GS/s sampling rate (i.e. samples are separated by 0.1 m of sampling resolution).

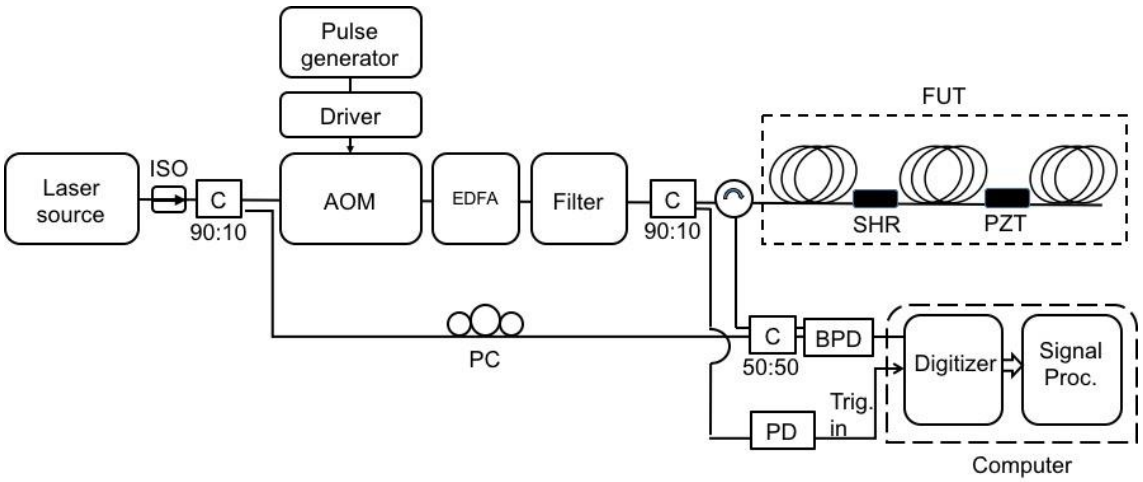

Figure 1:
Schematic of ϕ-OTDR system. ISO: Isolator, C: coupler, AOM: Acousto-optic modulator, EDFA: Erbium-doped fiber amplifier, SHR: Shaker, PZT: Piezo-electric transducer, FUT: Fiber under test, PC: Polarisarion controller, BPD: Balanced photo-detector, PD: Photo-detector.

The Fiber Under Test (FUT) is a cascade of three fiber drums, which are about 1.4 km, 1.3 km, and 2 km long, respectively (total length is about 4.7 km). Perturbations were applied at two different positions. A PZT (Piezo transducer) with 40 m of wound single mode fiber is located between 2320 and 2360 m along the sensing fiber as a vibration source in the system. The signal applied to drive the PZT is a sinusoidal wave (cf. Table 2 for PZT specifications), whose peak-to-peak voltage can be varied between 0 and 10 V and frequency adjusted from 200 Hz to 9kHz. Another vibration source used in the experiments was a shaker placed at 644 m where 2 m of fiber were glued 16 mm diameter plastic tube. The plastic tube was clamped at both ends, and the midpoint (corresponding to fiber position 644 m) was excited by a shaker to create the acceleration. The optical pulses with repetition rate of 19.964 kHz and pulse width of 100 ns are launched into the FUT. The complete list of parameters used in the experiments is given in Table 3.

Table 2. Piezo-electric transducer parameters used in the experiments

Piezo-Electric Transducer specification	Value
Modulation constant	23 radian/V @1.55 μm (up to 10 kHz)
Fiber stretch / optical delay	3.8 μm/V, 0.028 ps/V
Maximum voltage range	± 400V (800 V_{pp})

Table 3. System parameters used in the experiments

System Component	**Value**
Laser wavelength	1552.67 nm
Laser source power	40 mW
Laser Linewidth	0.1 kHz
Pulse peak power at the filter output	95 mW
AOM frequency shift (f_{AOM})	160 MHz
BW of the optical filter	0.9 nm
BW of the balanced detector	180 MHz
Fiber refractive index	1.468
Pulse Repetition Frequency (PRF)	19.964 kHz
Pulse duration	100 ns
Spatial resolution (resolution cell)	10 m
Length of FUT	4700 m
Vibration Location (PZT)	2320-2360m (40m)
Vibration Location (SHR)	644 m
Amplitude of PZT driver	1-10 V_{pp}
Number of resolution cell (‘*range bin*s’) /trace	450
Range bin of vibration location	227-230
Sampling frequency of digitizer	1GS/s
Number of sampled points/ OTDR trace, N	45000
Temporal processing interval (‘*slow time window*’)	30 ms
NEP of the balanced detector	0.3 pW/ $(Hz)^{1/2}$

2. MEASUREMENT RESULTS

As the probe signal (optical pulse launched into FUT) propagates along the fiber, the Rayleigh backscattered electric fields from the scattering centers within the resolution cell (i.e half the pulse width) interferes at the photodetector which results in an ϕ-OTDR trace representing a particular distribution of scattering centers along the resolution cell.

A typical ϕ-OTDR trace (amplitude R(t) in (2)) obtained by the experimental setup is shown in Figure 2. It consists of two sections; the first part is the Rayleigh backscattered signal up to the end of FUT having a decaying speckle pattern as expected, the second part represents the receiver noise (thermal noise and shot noise).

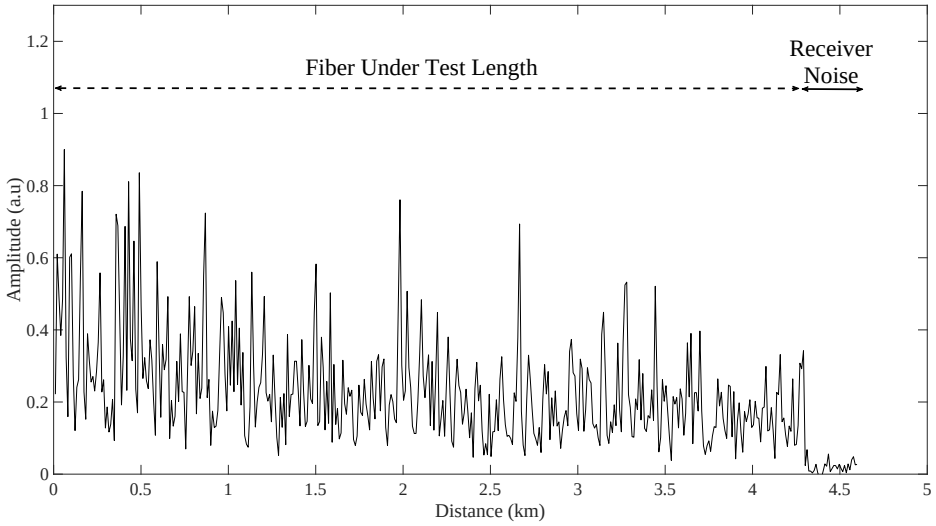

Figure 2:
A typical ϕ-OTDR trace recorded by the experimental test setup.

When a local perturbation is applied, relative positions of the scattering centers in the perturbed zone change as well as the local refractive index, resulting in a change on the measured power from that zone. For each measurement, 600 consecutive OTDR traces (number of records, $N_{rec} = 600$) were recorded. $N_{rec} - 1$ diffrence traces (ΔR_i) are formed by subtracting those 600 amplitude traces from the first one as

$$\Delta R_i = abs(R_{i+1} - R_i), i \in [1,\ N_{rec} - 1] \quad (3)$$

which will result in a peak around the point of perturbation, hence clearly points out the position of the applied vibration. As an example, 600 such differential traces are plotted in Figure 3 for PZT having f_{vib}=1.5 kHz. The amplitude response fluctuates significantly at the vibration position, whereas the fluctuation is relatively smaller at other positions.

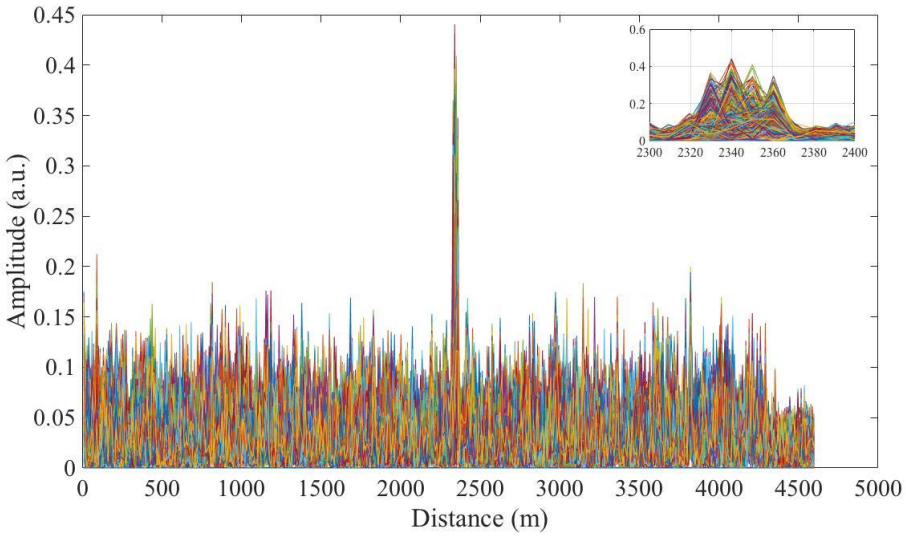

Figure 3:
Absolute values of amplitude differences ***Inset:*** *zoom on the PZT location.*

These differential amplitude signals can be put into a matrix form where each column represents the variation of the differential amplitude signals over the temporal processing interval ('*slow time window*' covering 600 consecutive traces) at a particular position. The representation of this matrix (i.e. slow-time versus distance where the differential amplitude is converted into the color range of 0 to 255) for the measurement of the previous example is shown in Figure 4. The obvious change around the vibration position is indicated inside the ellipse.

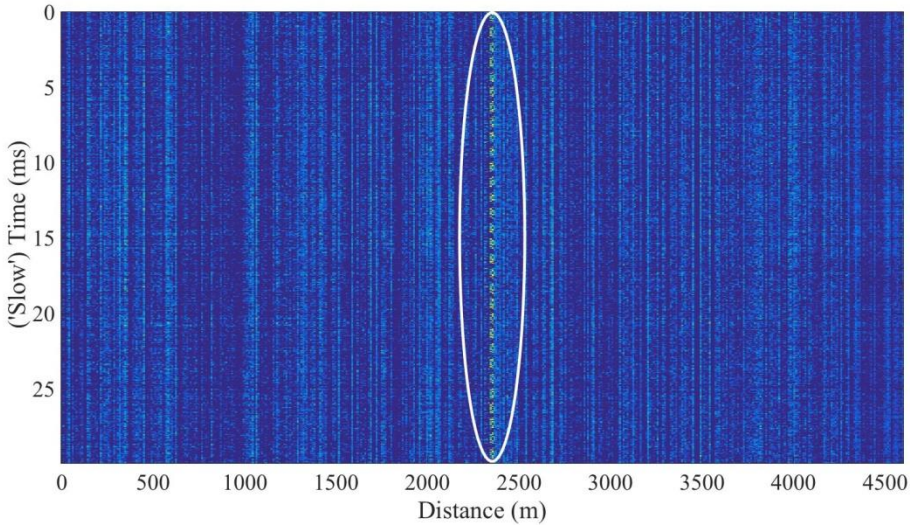

Figure 4:
Representation of slow-time versus distance for 600 consecutive ϕ-OTDR traces

Two rows taken from a vibration position (2360 m) and a non-vibration position (4200 m) along the fiber are compared in Figure 5. The amplitude value changes following the same rhythm of the applied vibration, whereas it remains relatively constant at a non-vibration position.

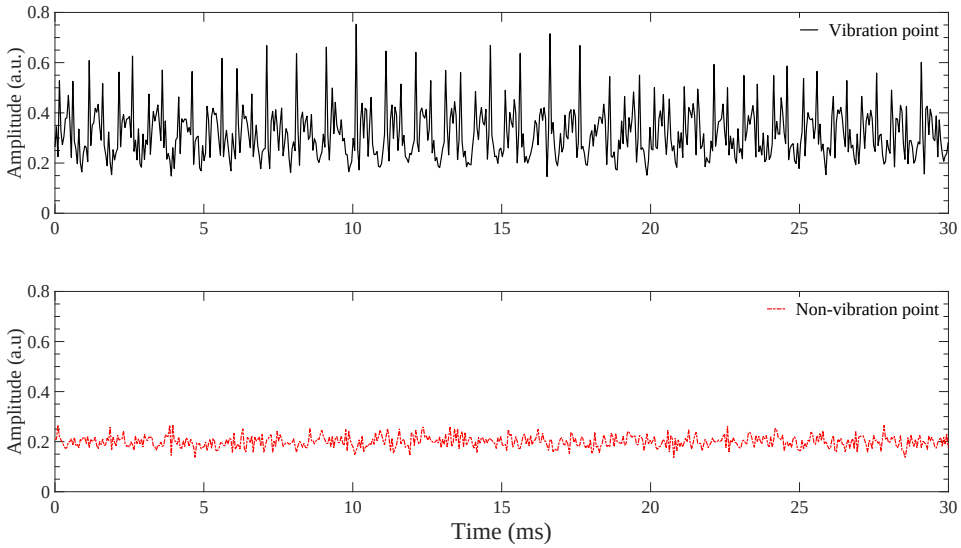

Figure 5:
Amplitude difference variation at the vibration (2360 m) and non-vibration (4200 m) positions.

2.1. Signal-to-Noise Ratio Calculations

The signal to noise ratio values of our ϕ-OTDR measurements have been calculated. For the SNR comparison measurements, a pulse peak power of 95 mW (after amplification and filtering) at the FUT input was used. The fiber was excited by the shaker using the arrangement as explained above. Two input signal amplitudes were used, resulting in two different accelerations (their ratio is 1:7). In each case, 14 measurements were made: no. 1 with no perturbation, measurements no. 2-7 correspond to frequencies 50, 100, 200, 400, 600 and 800 Hz, respectively, and measurements no. 8-14 correspond to frequencies 1, 2, 3, 4, 5, 6 and 6.9 kHz, respectively.

The signal-to-noise (SNR) for a single difference trace (ΔR_i) is defined according to the following equation:

$$SNR_{(i)} = 10\, log_{10}\left(\frac{\max(\Delta R_i[pert])}{rms(env(\Delta R_i[noise]))}\right), \quad i \in [1, N_{rec} - 1] \tag{4}$$

where $\max(\Delta R_i[pert])$is the maximum value of the difference trace within the perturbation zone and $rms(env(\Delta R_i[noise]))$ is the root-mean-square value of the envelope of the difference trace outside the perturbation zone (Jason, et.al., 2018).

For a number of difference traces, the mean SNR and the standard deviation can be used as a figure of merit representing the signal variation. In Figure 6 the SNR values of measurements with coherent detection are presented for both low and high signal setting of the shaker output. The seven-fold increase in the applied acceleration level resulted in higher SNR values (above 5 dB except 50 Hz, and 6.9 kHz).

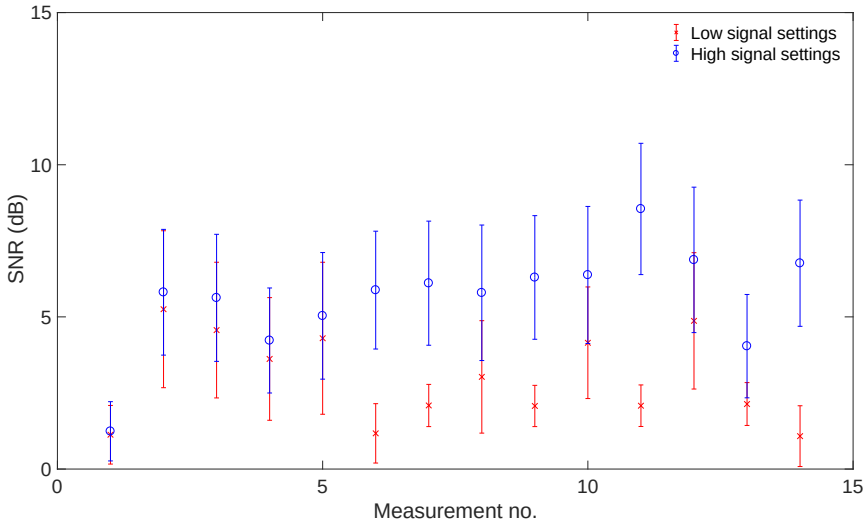

Figure 6:
Signal-to-noise for differential traces for low and high signal conditions.

2.2. Slow-time Analysis

The information of vibration location and frequency are generally separately extracted. Firstly, the location is detected as explained before (cf. Figure 3 and Figure 4). Then, the frequency information is obtained through FFT of the amplitude variation in the located vibration position. Figure 7 represents such variation at three different locations (at, before, and after the PZT position), for an example case for which the PZT (between 2320 and 2360 m) is driven by a sinusoidal signal having an amplitude of 3 V (A_{pzt}= 3 V) and frequency of 200 Hz. Vibration frequency is clearly extracted at the vibration position (together with a harmonic signal at 400 Hz), whereas the FFT amplitude doesn't include such frequency component at the two other non-vibration positions.

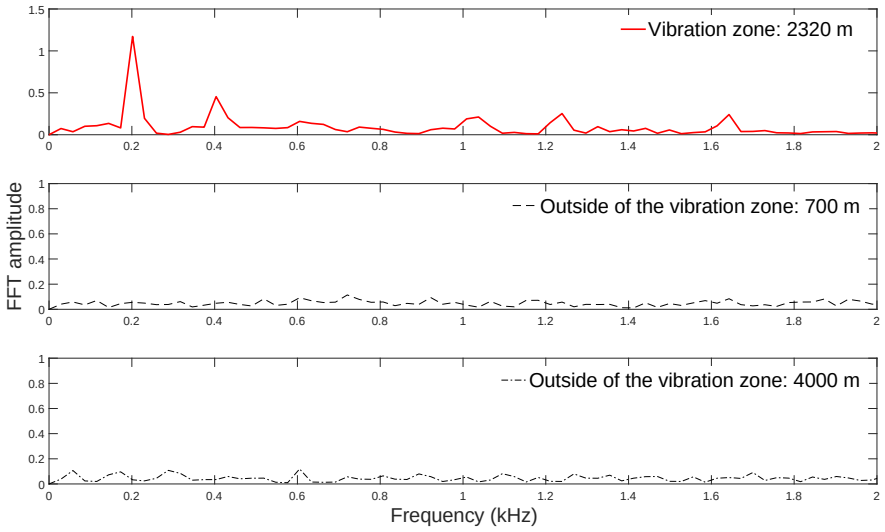

Figure 7:
Frequency spectrum for 600 consecutive phase-OTDR traces that is obtained based on amplitude of the traces (f_{vib}= 200 Hz, A_{pzt}= 3 V).

Vibration frequency can be extracted by using phase information as well. In the framework of the current paper, we demonstrated the mathematical development of the limitations on the maximum vibration frequency that can be determined by using phase information.

In this procedure, the phase calculation is performed along the fiber (fast-time) as

$$\theta_R(t) = unwrap\left[\arctan\frac{HT[I(t)]}{I(t)}\right] - 2\pi f_{AOM}t \tag{5}$$

where *HT* represents the Hilbert transform and *unwrap* means the result of an unwrapping algorithm. Then, differential phases ($\Delta\varphi = \theta_R(z_2) - \theta_R(z_1)$) are determined between neighboring locations (in general, with a distance of resolution cell). Finally, FFT analysis is applied on these differential phases at the perturbation location.

In the slow time analysis, the limitation imposed by the phase unwrapping algorithm can be expressed as

$$\left|\Delta\varphi\left(t + T_{pr}\right) - \Delta\varphi(t)\right| < \pi \tag{6}$$

where | | operator represents absolute value, T_{pr} stands for the pulse repetition period (the time between two successive pulses, T_{pr}=1/PRF). Assuming a periodic vibration which gives rise to a phase change having a maximum value of A_{ph}, and for a known pulse repetition rate, the maximum detectable vibration frequency that meets the requirement of (6) can be calculated as[†]

$$f_{max} < \frac{\pi}{2\,A_{ph}T_{pr}} \tag{7}$$

The relationship between the electrical signal applied on the PZT (A_{pzt}) and the corresponding phase change occurring in the optical signal (A_{ph}) can be calculated based on the specifications of the particular PZT used in the experiments (cf. Table 3). Equation (7) allows calculating the maximum vibration frequency (f_{max}) that can be detected by the ϕ-OTDR set-up for a particular A_{pzt}. Some example values are listed in Table 4 for the PZT used in our experiments.

Table 4. Maximum vibration frequencies calculated using equation 3 for various strain values (determined by the voltage applied on the PZT, A_{pzt}).

A_{pzt} (V)	A_{ph} (radian)	f_{max} (Hz)
3	133.8	234
2	89.2	350
1	44.6	703

In order to verify the requirement formulated in (7), a series of experiments have been realized. Figure 8 shows the results of these comparisons for an example case, where the vibration frequency of 500 Hz was successfully determined on the phase difference when

[†] Under the condition that $f_{vib} << 1/T_{pr}$

$A_{pzt} = 1\,V$ (f_{vib}< f_{max}=703 Hz), whereas 500 Hz frequency component could not be deduced for the other two amplitude values of 2 V and 3 V (f_{vib}> f_{max}).

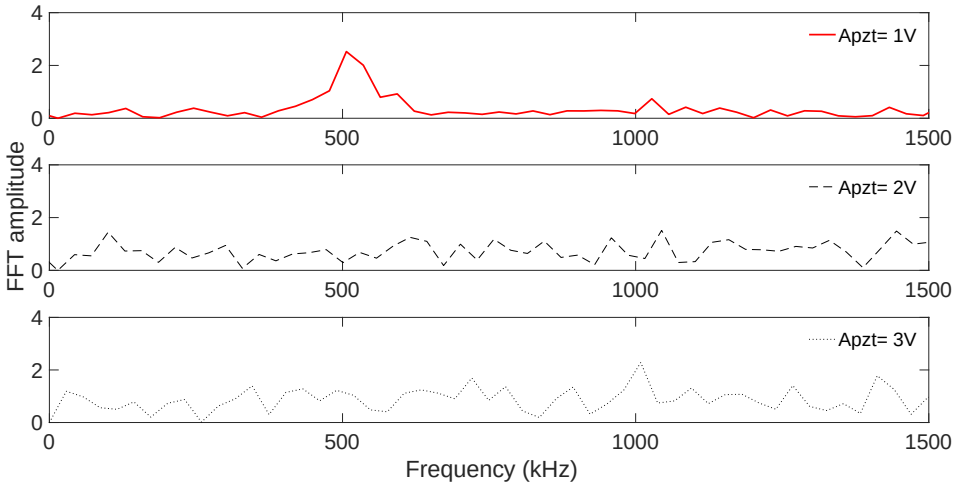

Figure 8:

Frequency spectrum for 600 consecutive phase-OTDR traces that is obtained based on phase difference of the traces for A_{pzt}= 1, 2, and 3 V (f_{vib}= 500 Hz).

The vibration frequencies obtained by the slow-time analysis on the amplitude and phase components of the measured signal are compared in Figure 9 and Figure 10 for two example cases.

As can be seen in Figure 9 and Figure 10, the harmonic frequency components observed on the amplitude response are successfully avoided by using phase difference traces in slow time analysis. For the vibration frequency of 200 Hz, the amplitude response contains unwanted frequency components at 50 Hz and 400 Hz (cf. Figure 9-b). Similarly, for the vibration frequency of 500 Hz the amplitude response gives rise to an unwanted frequency component at 1kHz (cf. Figure 10-b).

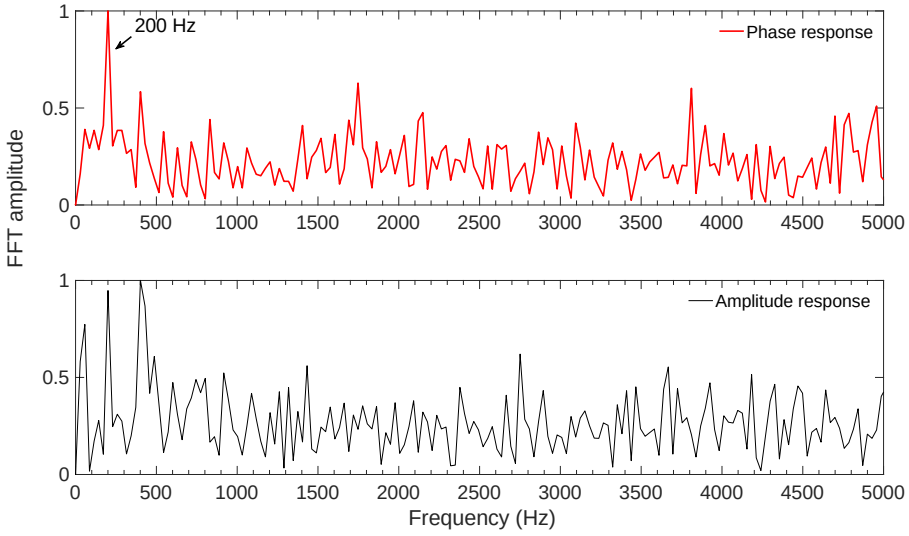

Figure 9:

Frequency spectrum for 600 consecutive phase-OTDR traces that is obtained based on phase difference and amplitude of the traces for A_{pzt}= 2 V (f_{vib}= 200 Hz).

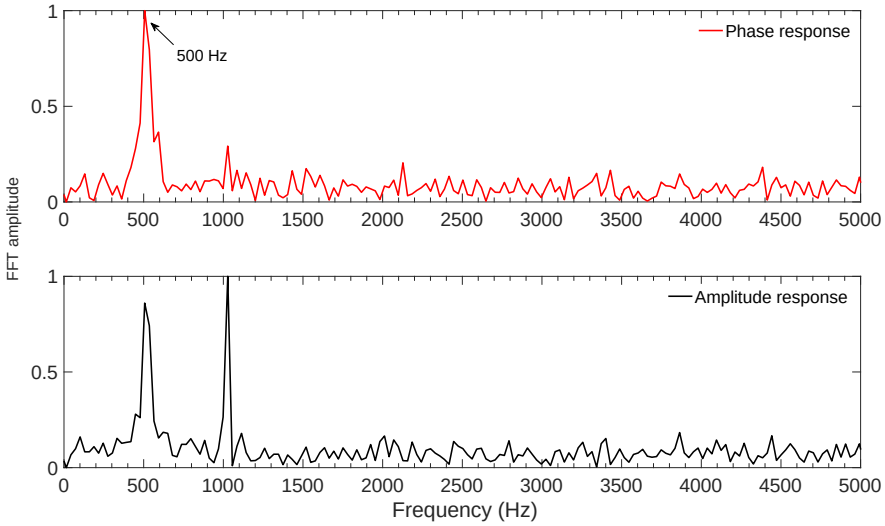

Figure 10:
Frequency spectrum for 600 consecutive phase-OTDR traces that is obtained based on phase difference and amplitude of the traces for A_{pzt}= 1 V (f_{vib}= 500 Hz).

3. CONCLUSION

In this work, a phase sensitive optical time domain reflectometer (ϕ-OTDR) prototype employing coherent detection scheme has been realized. An analysis algorithm has also been developed to calculate amplitude and phase evolution of the experimental phase-OTDR traces. Subtracting the amplitude traces from the reference trace (without perturbation) correctly indicated the position of the vibration for one, as well as two simultaneous vibration sources. Based on the measured traces, SNR values have been calculated and compared for different input signal amplitudes. Enhancement in SNR values (SNR above 5 dB except 50 Hz, and 6.9 kHz) has been obtained for a 7-fold increase in vibration amplitude. It was shown by the way experiments that, for a certain collection of difference traces, the maximum SNR, relative the noise reference level as defined in the paper, can be used as a measure of the ability to detect the perturbation.

Afterwards, slow-time analysis has been applied on both the amplitude and the differential phases. In spite of the fact that the vibration frequency is correctly determined by the FFT analysis of amplitude measurements, it is difficult to quantify the vibration amplitude (A_{pzt}). This is because there is no definite relationship between the measured amplitude and the vibration acceleration. In order to overcome this drawback, the phase information of recorded backscattering signal can be analyzed instead of the amplitude (Tu, et. al., 2015). The signal processing algorithm that has been elaborated in this work, however, focused on the determination of the vibration frequency rather than its amplitude. Thus, the slow-time analysis of the amplitude response and the phase difference were compared with respect to the appearance of unwanted harmonic frequencies. Slow-time analysis of the phase difference has been shown to be more reliable in avoiding harmonics, that can be considered as an important advantage in correctly interpreting the frequency spectrum obtained at the field measurements.

Finally, the limitations in slow-time analysis based on phase difference-distance traces have been formulated. In order to verify the requirement, a series of experiments have been realized for three different vibration amplitudes (A_{pzt} = 1, 2, 3 V), and 6 different vibration frequencies (f_{vib}= 50, 100, 200, 300, 500, 1000 Hz). The experimental validations were in excellent

agreement with the calculated limitations (e.g. maximum vibration frequency that can be measured for a given pulse repetition rate and phase amplitude configuration).

Acknowledgement

Kivilcim Yüksel gratefully acknowledges financial support from the Scientific and Technological Research Council of Turkey, (TUBITAK, BIDEB-2219-1059B191600612).

REFERENCES

1. Aktaş, M., Akgün, A., Demircin, M. U. and Büyukaydın, D. (2017) Deep learning based multi-threat classification for phase-OTDR fiber optic distributed acoustic sensing applications, *Proc. SPIE 10208, Fiber Optic Sensors and Applications XIV, 102080G*, doi: 10.1117/12.2262108

2. He, H., Shao, L. Y., Li, Z., Zhang, Z., Zou, X., Luo, B., Pan, W. and Yan, L. (2016) Self-Mixing Demodulation for Coherent Phase-Sensitive OTDR System, *Sensors*, 16(5), 681, doi:10.3390/s16050681

3. Jason, J., Yüksel, K. and Wuilpart, M. (2017), Laboratory evaluation of a phase-OTDR setup for railway monitoring applications, *IEEE Photonics Society, Annual Symposium*, Delft, pp 18-21

4. Jason, J., Popov, S. M., Butov, O. V., Chamorovskiy, Y. K., Golant, K. M., Fotiadi, A. A. and Wuilpart, M. (2018) Sensitivity of high Rayleigh scattering fiber in acoustic/vibration sensing using phase-OTDR, *SPIE Photonics Europe*, Strasbourg, Vol. 10680, doi:10.1117/12.2307569

5. Juarez, J. C., Maier, E. W., Choi K. N. and Taylor, H. F. (2005) Distributed Fiber-Optic Intrusion Sensor System, *J. of Lightwave Technology*, 23(6), 2081-2087. doi**:**10.1109/JLT.2005.849924

6. Lu, Y., Zhu, T., Chen, L. and Bao, X. (2010) Distributed Vibration Sensor Based on Coherent Detection of Phase-OTDR, *J. of Lightwave Technology*, 28(22), 3243-3249. doi**:**10.1109/JLT.2010.2078798

7. Liu, Y., Liu, X., Jin, B., Bai, Q., Wang, Y., Wang, D., Wang, Y. (2016) Distributed Fiber-Optic Sensors for Vibration Detection", *Sensors*, 16(8), 1164. doi:10.3390/s16081164

8. Madsen, K. N., Thompson, M., Parker, T. and Finfer, D. (2013) A VSP field trial using distributed acoustic sensing in a producing well in the North Sea, *74thEAGE Conference & Exhibition, Extended Abstracts*, 31(11), 51-56. doi:10.3997/1365-2397.2013027

9. Maral, H., Akgun, T. and Aktas, M. (2018), Adaptive power thresholding for real time threat detection in distributed acoustic sensing systems, *26thSignal Processing and Communications Applications Conference (SIU)*, 2-5 May, Izmir. doi:10.1109/SIU.2018.8404671

10. Miah, K., Potter, D. K. (2017) A Review of Hybrid Fiber-Optic Distributed Simultaneous Vibration and Temperature Sensing Technology and Its Geophysical Applications, *Sensors*, 17, 2511. doi:10.3390/s17112511

11. Olcer, I. and Oncu, A. (2017) Adaptive temporal matched filtering for noise suppression in fiber optic distributed acoustic sensing, *Sensors*, 17(6), 1288. doi: 10.3390/s17061288

12. Pan, Z., Liang, K., Ye, Q., Cai, H., Qu, R. and Fang, Z. (2011), Phi-OTDR system based on digital coherent detection, *Proc. of SPIE-OSA-IEEE Asia Communications and Photonics*, 8311. doi:10.1364/ACP.2011.83110S

13. Peng, F., Wu, H., Jia, X. H., Rao, Y. J., Wang Z. N. and Peng, Z. P. (2014) Ultra-long high-sensitivity phase-OTDR for high spatial resolution intrusion detection of pipelines, *Opt. Express*, 22(11), 13804-13810. doi:10.1364/OE22.013804

14. Ren, M., Ping, L., Chen, L. Y. and Bao, X. (2016) Theoretical and experimental analysis of Phi-OTDR based on polarization diversity detection, *Photonics Technology Letters*, 28(6), 697-700. doi:10.1109/lpt.2015.2504968

15. Taylor, H.F (1993), Apparatus and Method for Fiber Optic Intrusion Sensing, U.S. 5194847 A, 16 March 1993.

16. Tu, G., Zhang, X., Zhang, Y., Zhu, F. Xia, L. and Nakarmi, B. (2015) The development of an Phi-OTDR system for quantitative vibration measurement, *IEEE Photonics Technol. Lett.*, 27(12), 1349-1352. doi:10.1109/LPT.2015.2421354

17. Yu, M., Liu, M., Chang, T., Lang, J., Chen, J. and Cui, H. L. (2017) Phase-sensitive optical time-domain reflectometric system based on a single-source dual heterodyne detection scheme, *Applied Optics*, 56(14), 4058-4064. doi:10.1364/AO.56.004058

18. Wang, Z., Lu, B., Zheng, H., Ye, Q., Pan, Z., Cai, H., Qu, R., Fang, Z. and Zhao, H. (2017) Novel Railway-Subgrade Vibration Monitoring Technology Using Phase-Sensitive OTDR, *25th International Conference on Optical Fiber Sensors*, *Proc. of SPIE*, South Korea, 10323. doi:10.1117/12.2265169